JOURNAL OF MATERIALS SCIENCE **35** (2000) 555–566

Toughening and strengthening of polypropylene using the rigid-rigid polymer toughening concept

Part II *Toughening mechanisms investigation*

GUANG-XUE WEI, H.-J. SUE*
Polymer Technology Center, Department of Mechanical Engineering, Texas A&M University, College Station, TX 77843-3123
E-mail: hjsu@acs.tamu.edu

J. CHU
Visteon Automotive System, Dearborn, MI 48121

CHENGYA HUANG, KECHENG GONG
Department of Polymer Material Science and Technology, South China University of Technology, Guangzhou, Guangdong 545007, People's Republic of China

Toughening mechanisms in blends of isotactic polypropylene and Noryl polyphenylene oxide/polystyrene (iPP/Noryl) are studied using optical microscopy, scanning electron microscopy and transmission electron microscopy. Large Noryl particles (10–15 μm) are formed in iPP/Noryl blend and crazing is found to be the dominant toughening mechanism. A detailed investigation of fracture mechanisms reveals that Noryl particles help trigger and stabilize massive crazes in the iPP matrix. Incorporation of a small amount of styrene-ethylene-propylene (SEP) compatibilizer helps reduce Noryl particle size and improve interfacial adhesion between iPP and Noryl particles. Crazing and shear banding mechanisms are found to operate sequentially in iPP/Noryl/SEP blends. As a result, significantly improved toughness is obtained.

1. Introduction

The increasing market demands for structural applications of polypropylene (PP) have triggered extensive research on improving impact strength and reducing notch sensitivity of PP. A widely employed strategy for improving the toughness of single phase thermoplastics has involved the incorporation of an elastomeric phase. A disadvantage of such addition is that it reduces modulus and tensile strength, which are important benchmarks for acceptable material performance. To improve toughness while maintaining stiffness of thermoplastics, the rigid-rigid polymer toughening concept [1–6] has been introduced and shown to be a promising approach. Examples of these rigid-rigid polymer pairs are polybutylene terephthalate/polycarbonate (PBT/PC), nylon 6,6/polyphenylene oxide (PA/PPO), acrylonitrile-butadiene-styrene/polycarbonate (ABS/PC), and nylon 6,6/acrylo-nitrile-butadiene-styrene (PA/ABS) [7–9]. These rigid-rigid polymer blends exhibit a desirable combination of mechanical and physical properties of the constituents. Depending on the composition of the polymer pair utilized, however, the rigid-rigid polymer blends are not necessarily tough [7]. In fact, blending two or more randomly chosen rigid polymers will usually result in blends with poor and unpredictable properties.

To increase the toughness of a given polymer, the material needs to be engineered to possess effective energy dissipating processes. For thermoplastics, massive crazing and shear yielding are the most frequently encountered fracture energy dissipation processes. These two energy adsorbing processes are not mutually exclusive micromechanisms. In many polymers both may occur sequentially [3] or simultaneously [10–12]. The requirements for crazing and shear banding to operate effectively were extensively discussed in literature [13–17]. In rubber toughened polymers, a commonly accepted view on the role of rubber particles is that the rubber inclusions alter the stress state in the material around the particles through rubber cavitation and induce extensive plastic deformation. For neat PP, it is found that crazing is the main fracture energy dissipating process [18–20]. In the case of rubber-toughened PP, crazing and shear yielding are found to be the two most important fracture mechanisms [21–27]. If rigid thermoplastic particles in PP matrix can play the roles similar to rubber particles, it is likely that PP can be effectively toughened *via* either massive crazing and/or shear banding without sacrificing stiffness.

The concept of rigid-rigid polymer toughening is not new. The main fracture mechanisms reported in rigid-rigid polymer blends that contain an elastomeric phase

* Author to whom all correspondence should be addressed.

are crazing followed by shear banding [3] and rubber phase cavitation followed by shear yielding [28, 29]. On the other hand, Nair *et al.*, and Majumdar *et al.*, found that addition of the second phase rigid polymer results in embrittlement of Nylon 6,6/ABS [7–9] and Nylon 6/ABS [29]. They attributed the poor toughness to poor interfacial adhesion between the matrix and the toughener phase. However, it is still not clear why toughness is increased in some blends and not so in others. The role of particle size and interfacial adhesion in toughening is still not well understood. To answer these questions and to establish a criterion for the development of toughened polymer blends, it is imperative that one fully understand the fundamental parameters that govern fracture in rigid-rigid polymer blends. Specifically, the sequence of toughening events and the role(s) that the toughener phase plays with respect to each operative microscopic mechanism has to be known when polymer fractures. Moreover, damage events should be linked to material characteristics, such as particle phase morphology, particle size, interfacial adhesion, and crystallinity.

In Part I of this series [30], the morphology and toughness of iPP/Noryl and iPP/Noryl/SEP blends were reported. It was shown that the presence of a rigid polymer in iPP matrix significantly improved the toughness of iPP without causing any reduction in the modulus of iPP. The addition of a small amount of SEP compatibilizer, which helps reduce Noryl particle size and increase interfacial adhesion between iPP and Noryl particles, further increased the toughness of iPP.

The current study is part of a larger effort to gain an insight into some fundamental issues on rigid thermoplastic toughened iPP: Do Noryl particles play a similar role(s) in iPP/Noryl blends to those of rubber particles in PP/rubber blends? If not, what are the differences? Can the Noryl particles alter the toughening process in PP? And how? What is the strategy for making a tough and stiff polymer system *via* the rigid-rigid polymer toughening concept? This study attempts to answer these questions through the investigations of fracture mechanisms. A number of techniques, such as double notch four-point bending (DN-4PB) technique, scanning electron microscopy (SEM), transmission electron microscopy (TEM), and optical microscopy (OM), were employed to investigate the deformation mechanisms in iPP/Noryl and iPP/Noryl/SEP blends. It is anticipated that the results from this study will be beneficial to the development of other toughened rigid-rigid polymer alloys.

2. Experimental

2.1. Materials

The PP used to conduct this research is isotactic PP (iPP) that has an $M_n = 100{,}000$ and $M_w = 368{,}000$ with a melt flow rate index (MFI) of 2.5. The Noryl PPO/PS pellets, Noryl™ PX0844, which has a glass transition temperature (T_g) of 150 °C, were supplied by General Electric Company. The PS phase contains an undisclosed amount of rubber. The reason that this Noryl system was chosen was to allow the processing of the blends at 200 °C. The styrene-ethylene-propylene (SEP) (Kraton-G1701) diblock copolymer, which was used as a compatibilizer, was obtained from Shell Chemical. All polymers used in this research are commercial products. Blends of iPP/10%Noryl, iPP/10%Noryl/2%SEP, and iPP/10%Noryl/5%SEP were prepared using a research grade roll milling machine at a roll temperature of 200 °C.

2.2. Specimen preparation

The iPP, iPP/10%Noryl, iPP/10%Noryl/2%SEP, and iPP/10%Noryl/5%SEP blends were compression molded into 4 mm thick sheets at 200 °C. Cooling water was used to quickly cool the plaques. DN-4PB specimens were cut from the compression molded plaques. Samples were machined into dimensions of 63.5 mm × 12.7 mm × 4.0 mm. The DN-4PB bars were first notched with a 250 μm radius notch cutter to a depth of 3.75 mm and then further sharpened by wedging open a crack with a fresh razor blade which had been cooled in liquid nitrogen. This procedure ensures that a sharp crack tip is created. During DN-4PB specimen preparation, efforts were made to ensure that the cracks generated were as nearly equal in length as possible.

The DN-4PB specimens were tested at 50.8 mm/min using a screw-driven mechanical testing machine (Instron Model 4411) at room temperature. During the test, care was taken to ensure that the two inner loading points contacted the specimen simultaneously while the specimen was supported at the outer loading points.

2.3. Microscopy

The DN-4PB damage zone of the subcritically propagated crack was cut along the crack propagation direction but perpendicular to the fracture surface using a diamond saw. The plane-strain core region of the crack tip damage zone was prepared for TOM, SEM, and TEM investigations.

In the TOM investigation, about 30 μm thin sections of the tested DN-4PB samples were obtained by polishing, following the procedure described by Holik *et al.* [31]. The thin sections were then examined using an Olympus BX60 optical microscope under both bright field and cross-polarization conditions.

SEM investigations were performed on polished DN-4PB tested specimens to investigate the toughening mechanisms. In this experiment, the specimen was polished following the same procedure as that in the TOM investigation to obtain flat and smooth surfaces. The polished specimen was subsequently immersed in a solution containing 1.3 wt% $KMnO_4$, 32.9 wt% dry H_3PO_4 and 65.8 wt% H_2SO_4 for 24 hrs [32, 33]. SEM was also performed on the fracture surface to observe evidence of interfacial adhesion. All specimens were coated with a 30 nm layer of Au-Pd and investigated using JSM-6400 SEM operated at an accelerating voltage of 15 kV.

For the TEM experiments, specimens were carefully trimmed to an appropriate size (an area of 5 × 5 mm)

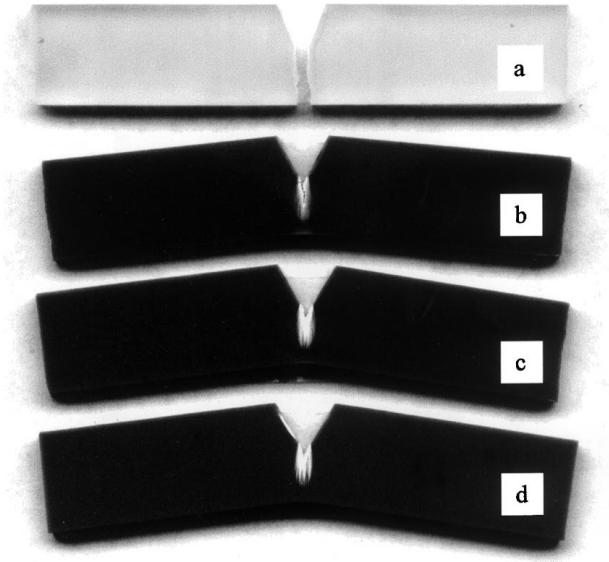

Figure 1 Fracture patterns of iPP and Noryl-toughened iPP: (a) Neat iPP, (b) iPP/10%Noryl, (c) iPP/10%Noryl/2%SEP and (d) iPP/10% Noryl/5%SEP. Large plastic deformation zone is observed in Noryl-toughened iPP blends.

and embedded in DER 331 epoxy/diethylenetriamine (12 : 1 ratio by weight). The epoxy mount was cured at room temperature overnight. The cured block was further trimmed to a size of about 0.3×0.3 mm. A diamond knife was used to face off the trimmed block prior to RuO_4 staining. The faced-off block was exposed to the vapor of an aqueous RuO_4 solution (0.5% by weight) for 2.5 hrs. Ultra-thin sections, ranging from 60 to 80 nm, were obtained using a Reichert-Jung Ultracut E microtome with a diamond knife at room temperature. The thin sections were placed on 200-mesh formvar-coated copper grids and examined using a JEOL 2000FX ATEM operated at an accelerating voltage of 100 kV.

3. RESULTS

3.1. General view of fracture patterns

The fractured SEN-3PB specimens are shown in Fig. 1. It is observed that neat iPP experiences a brittle behavior with little sign of plasticity. The crack propagates unstably once it starts. With an addition of 10% by weight of Noryl particles, a pronounced damage zone forms and the crack experiences stable growth during loading. This indicates that addition of Noryl particles improves fracture toughness and increases the crack propagation resistance of iPP. As for the iPP/Noryl/SEP blends, the samples show a more intense and a larger damage zone than that in iPP/Noryl blend. Also, the crack growth is further delayed by incorporating SEP, suggesting that SEP can effectively alter the fracture process. All the above fracture processes are consistent with the load-displacement curves reported previously [30]. From this simple test, it is noted that rigid Noryl particles and SEP both play an important role in the toughness improvement of iPP. To unambiguously understand the roles that Noryl particles and SEP play in toughening, TOM, SEM, and TEM investigations are conducted on DN-4PB specimens of iPP, iPP/10%Noryl, iPP/10%Noryl/2%SEP, and iPP/10%Noryl/5%SEP blends.

3.2. Fracture behavior of neat iPP

For comparison purposes, the fracture mechanism of neat iPP was first studied using TOM. The micrographs of DN-4PB tested specimen are shown in Fig. 2. As expected, a small damage zone is developed around the crack tip. It appears that crazing is the only energy dissipating process. No birefringence is found in the crack tip damage zone (Fig. 2b). When the specimen is examined at a higher magnification, it is observed

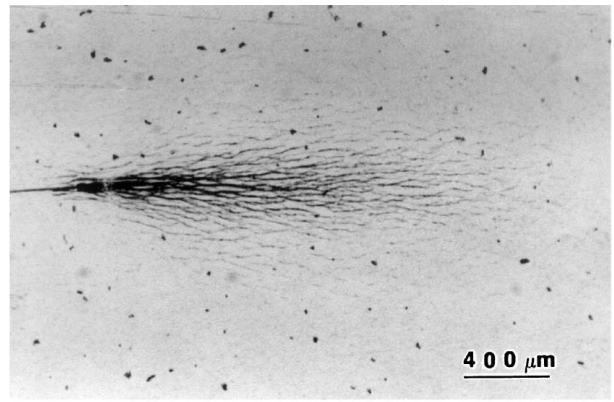

(a)

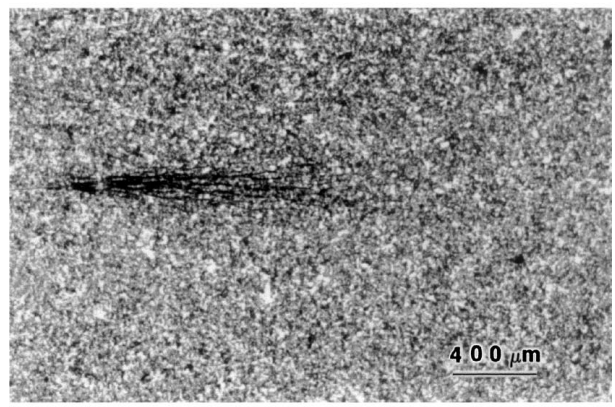

(b)

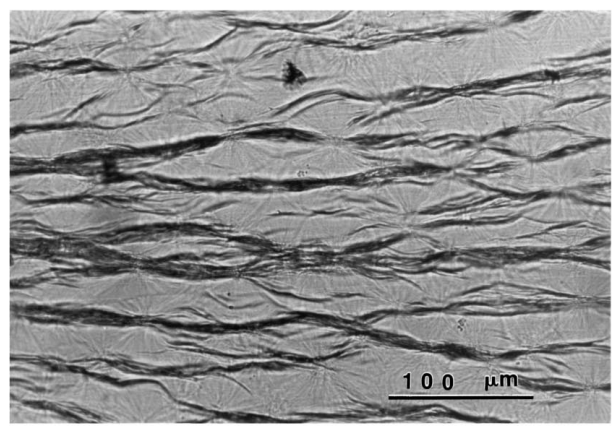

(c)

Figure 2 TOM of DN-4PB neat iPP specimen: (a) Taken under bright field, (b) cross-polarized light, and (c) high magnification under bright field light. No birefringence is found (see b). Crazes go through centers and boundaries of spherulites (see c). The crack propagates from left to right.

that crazes go through the boundaries and centers of spherulites (Fig. 2c). With further loading, the main craze is easily developed into a crack. This deformation mechanism is consistent with the low toughness value reported earlier [30].

3.3. Toughening mechanisms in iPP/Noryl blend

As expected, the TOM photographs of the DN-4PB tested specimen of the iPP/Noryl blend clearly reveal that massive crazes formed around the crack tip damage zone (Fig. 3a). However, no birefringence is observed when the specimen is examined under cross-polarized light (Fig. 3b). This damage phenomenon is similar to that observed in neat iPP. However, the size of damage zone and the level of crazing in iPP/Noryl blend are much higher than that in neat iPP. It is apparent that the observed crazes are associated with Noryl particles when the specimen is viewed at a higher magnification (Fig. 3c). Most crazes appear to be initiated from and terminated at the Noryl particles. The Noryl particles may act as stress concentrators to trigger crazes and stabilize the growing crazes.

The TEM investigation performed in the sub-fracture surface zone clearly shows that massive crazes are generated (Fig. 4). Large crazes are found between particles (Fig. 4a), and seem unorganized due to the irregularly shaped Noryl particles and the presence of spherulites in iPP matrix. Particle debonding from matrix is also observed in this region, indicating that interfacial bonding is not strong. Nevertheless, Noryl particles appear to be effective in generating massive crazes (Fig. 4b). TEM micrographs taken at 50 μm beneath crack surface (Fig. 4c) and 200 μm ahead of crack tip (Fig. 4d) show sparse and small crazes. No obvious debonding is observed in these regions, which indicates that even through the interfacial bonding between iPP and Noryl particles is not strong, it is enough for triggering crazes.

3.4. Toughening mechanisms in iPP/Noryl/SEP blends

Large Noryl particles (about 10–15 μm) are formed in iPP/10% Noryl blend, which limit the fracture mechanism mainly to crazing. Addition of SEP compatibilizer into iPP/Noryl blend dramatically reduces the Noryl particle size and appears to form a core-shell particle phase morphology in iPP/10%Noryl/SEP blends as reported in Part I [30] of this series. The resistances to crack initiation and crack propagation are significantly increased by addition of a small amount of SEP.

Two levels of SEP compatibilizer, i.e., 2% and 5% by weight, were used to compatibilize iPP/10%Noryl blend. First, we focus on iPP/10%Noryl/5%SEP blend, and then show similarities and differences between the two blends.

When 5% SEP is added into iPP/10%Noryl blend, the damage mechanisms are dramatically changed. As shown in Fig. 5, the TOM micrographs of the DN-4PB specimen clearly indicate the presence of a cavitation zone (Fig. 5a) and a birefringent zone (Fig. 5b) in the crack tip region. This birefringent zone, which is an indication of shear banding, is encompassed by a large light scattering cavitation zone. These interesting deformation features were further studied using TEM.

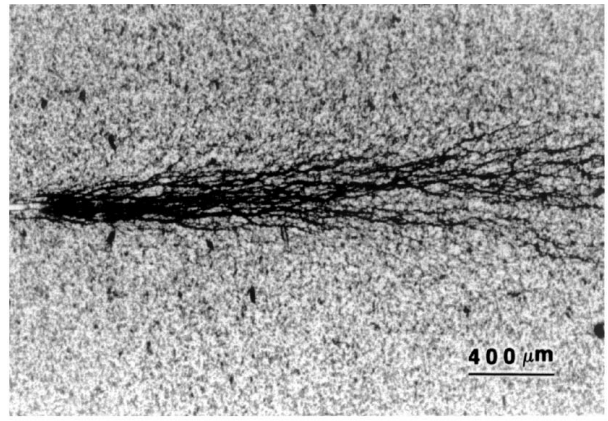

(a)

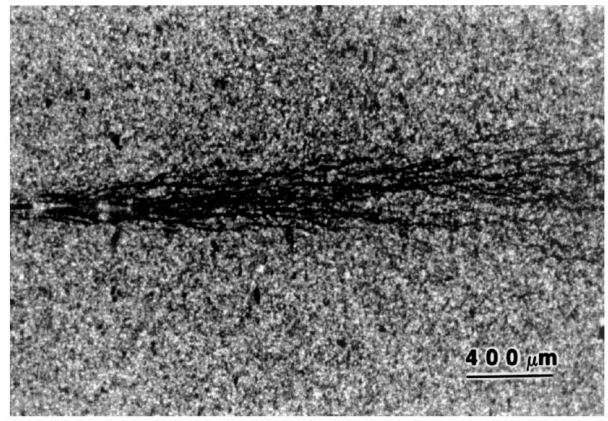

(b)

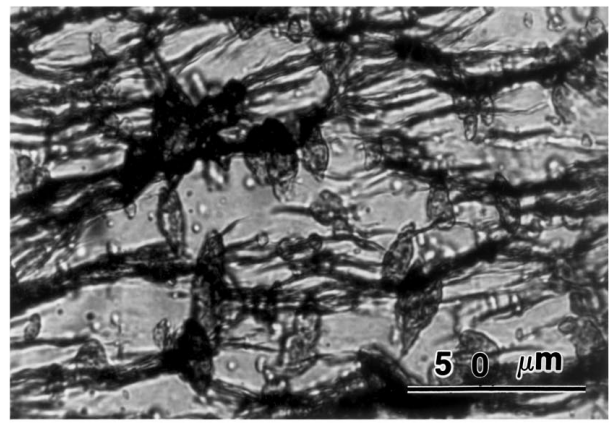

(c)

Figure 3 TOM of DN-4PB iPP/10%Noryl specimen taken under (a) bright field, (b) cross-polarized light, and (c) high magnification in craze zone. Most crazes are associated with Noryl particles (see c). The crack propagates from left to right.

TEM micrographs in Fig. 6 were taken in the crack wake at different strata on DN-4PB tested iPP/10% Noryl/5%SEP specimen. The sequence of deformation events can be studied here. In the crazed zone, i.e., about 100 μm beneath the fracture surface, massive crazes are found in the iPP matrix (Fig. 6a). Particles in this region have the same shape as that in the undamaged region (Fig. 6f) and hence there is no observable

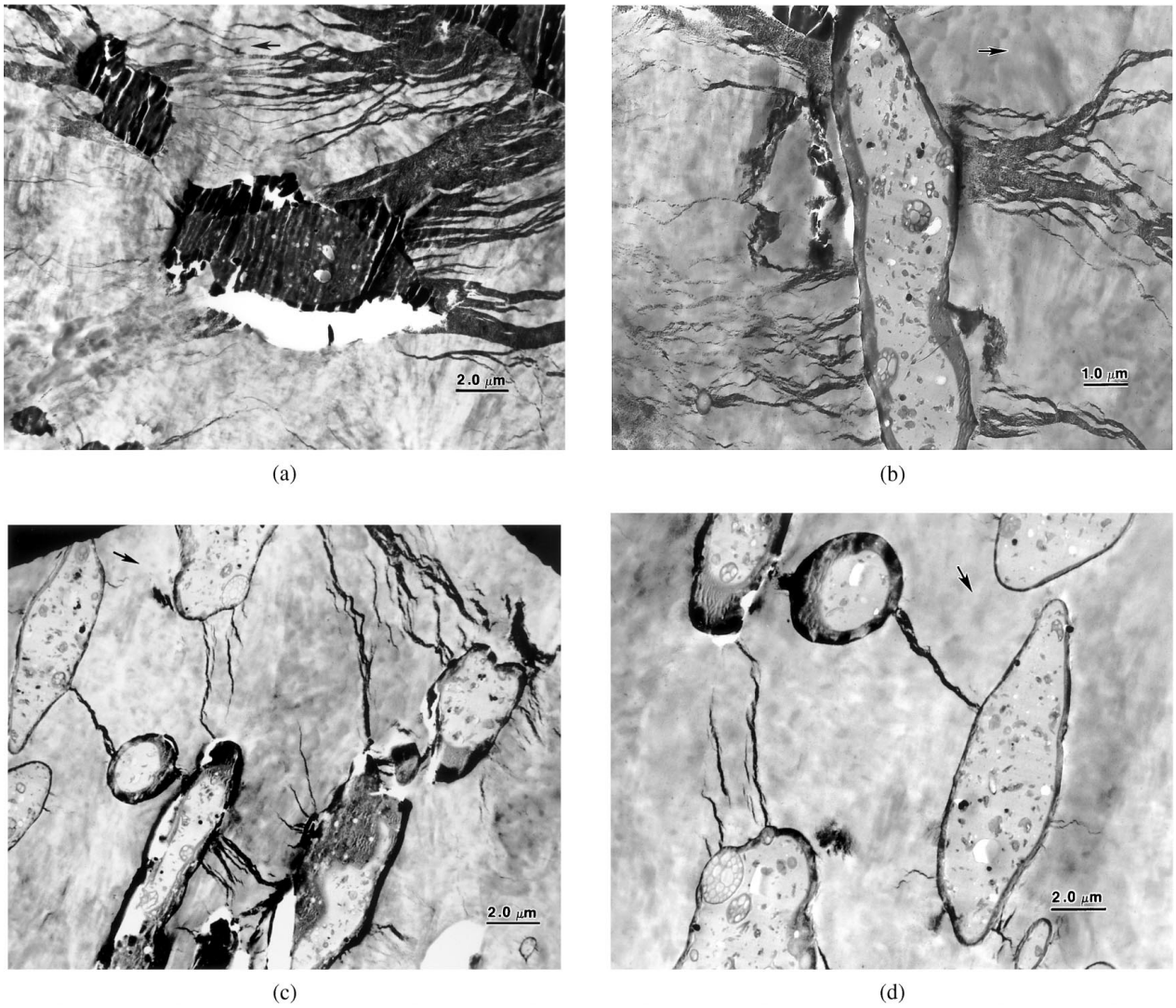

Figure 4 TEM micrographs of DN-4PB iPP/10%Noryl thin section taken from various regions around the crack. In (a) and (b), massive crazes are generated by Noryl particle immediately beneath the crack surface; in (c) 50 μm beneath the crack surface and (d) 200 μm ahead of the crack tip, sparse crazes associated with Noryl particles are still observed. The arrow indicates crack propagation direction.

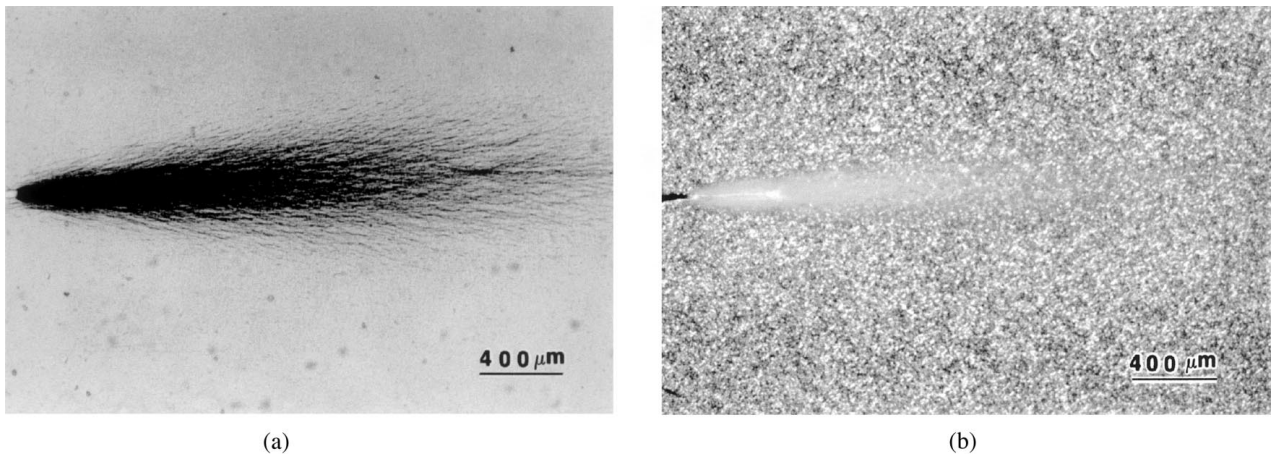

Figure 5 TOM of DN-4PB iPP/10%Noryl/5%SEP specimen taken under (a) bright field and (b) cross-polarized tight. The crack propagates from left to right.

shear deformation in the matrix at this stage. This is the first stage of the deformation sequence. Fig. 6b, taken at around 50 μm beneath crack surface, shows the second stage in the sequence. This stage consists of distorted particles in the loading direction (indicated by tails at equator of particles), implying that the iPP matrix around the distorted particles has undergone shear yielding to some extent. The proof of extensive shear deformation of the matrix material is demonstrated in Fig. 6c, d, and e which were taken immediately beneath

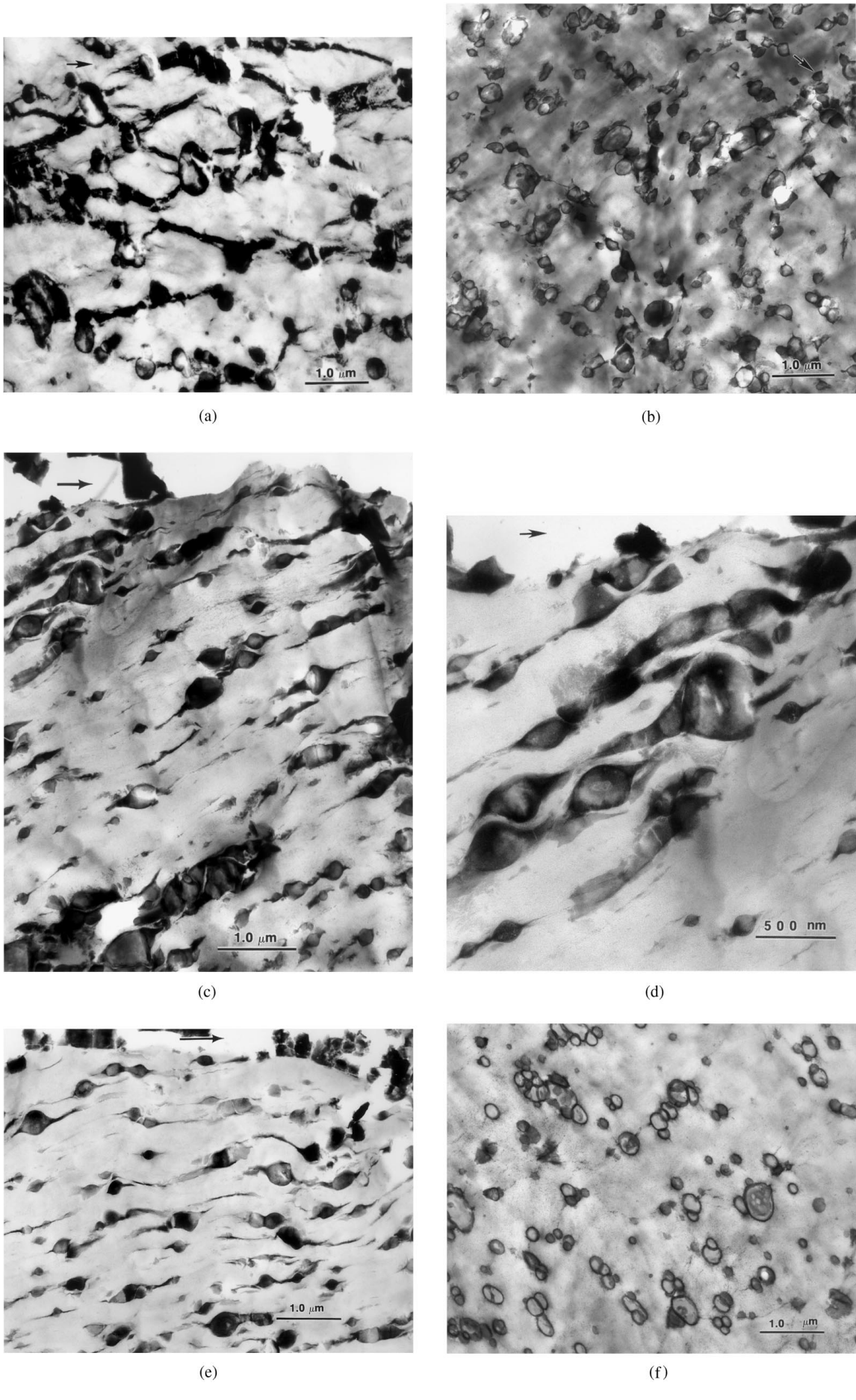

Figure 6 TEM micrographs of a DN-4PB iPP/10Noryl/5%SEP thin section taken from various regions in the crack wake. (a) 100 μm beneath the crack surface, (b) 50 μm beneath the crack surface, (c), (d) immediately beneath the crack surface, close to the crack tip, (e) immediately beneath the crack surface but 200 μm behind the crack tip, and (f) undamaged region. The arrow indicates crack propagation direction.

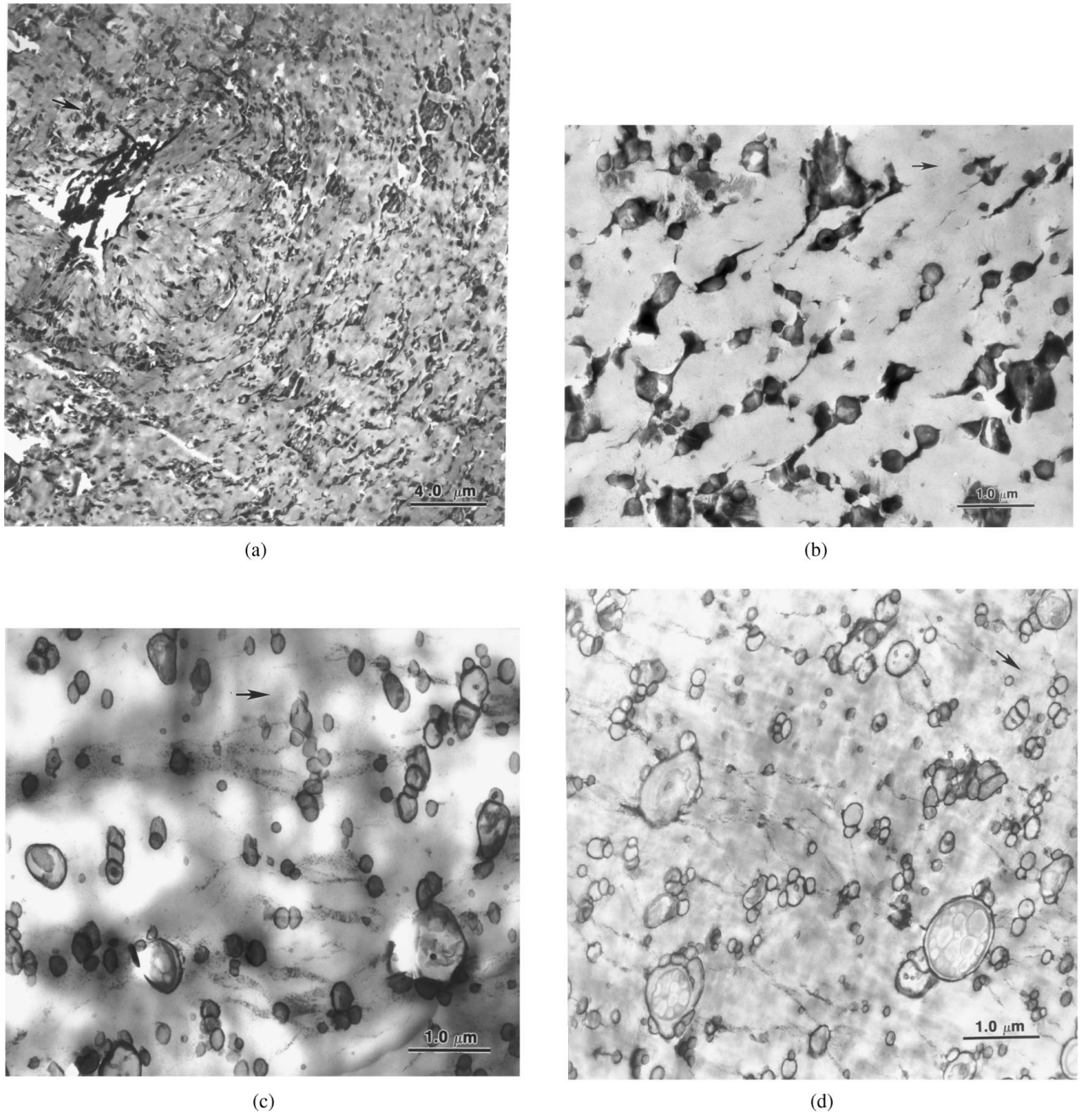

Figure 7 TEM micrographs of a DN-4PB iPP/10%Noryl/5%SEP thin section taken from various regions around crack tip. (a) At crack tip, (b) 50 μm ahead of the crack tip, (c) 150 μm and (d) 300 μm ahead of the crack tip. The arrow indicates crack propagation direction.

the fracture surface. Highly deformed particles are observed inside this region, suggesting that plastic deformation has occurred. Very short and narrow crazes are also visible in this region. The crazes appear to be distorted by the shear yielding process. A careful investigation of the micrograph reveals that the interfacial layers, which mainly consist of SEP compatibilizer (indicated by a dark color due to staining), are highly elongated (see tails in the equator of particles) while the cores of the particles remain almost undeformed (Fig. 6d). The elongation direction is at an angle of about 30° to 40° with respect to crack growth direction in the region close to the crack tip (Fig. 6c and d). This angle decreases with increasing distance behind the crack tip (Fig. 6e). The tail lengths at the equator of the particles exhibit a decreasing elongation and alignment with respect to the crack surface away from the fracture surface (Fig. 6c). This finding is consistent with the work on PA/PPO [3].

TEM investigations reveal complex deformation features in regions ahead of the crack tip (Fig. 7a). Again, crazes are distorted as those observed in Fig 6c. The matrix material in the region near the crack tip experiences large scale stretching (Fig. 7a). Obviously, diffuse shear yielding occurs in this region. The fan-shape deformation zone is caused by crack tip stretching and unloading. At approximately 50 μm ahead of the crack tip, Fig. 7b, the length of the tails at the equator of the particles is smaller compared to that at the crack tip (Fig. 7a) and the crack wake (Fig. 6c). This feature is similar to that observed in the transition region of the crack wake (Fig. 6b). Only a few crazes are observed in this region. Further ahead of the crack tip, i.e., at 150 μm and 300 μm, respectively, only crazes are

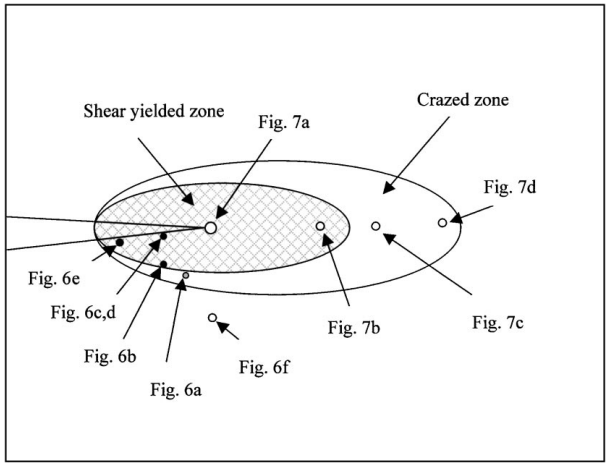

Figure 8 A schematic of the deformation features in the damaged DN-4PB iPP/10Noryl/5%SEP specimen. The location of TEM micrographs shown in Figs 6 and 7 are indicated in this drawing. Note that the features are not drawn to scale.

observed (Fig. 7c and d). The crazes become thinner and smaller with increasing distance away from the crack tip. Most crazes appear to be linked to Noryl particles. No signs of matrix stretching or tails at the equator of particles are found. A schematic drawing of the locations chosen for TEM investigation is shown in Fig. 8.

The Noryl particles appear to be effective in triggering crazes and preventing them from developing into premature cracks. Upon further loading, shear banding begins to take place due to the relief of triaxial tension by extensive crazing in the crack tip region. It is interesting to note that Noryl particles at this small size ($\approx$0.3 μm) are still effective in triggering crazes. A transformation of toughening mechanism from crazing to shear banding has clearly taken place in this blend. This is similar to that observed by Sue and Yee [3] in PA/PPO alloy.

The morphological studies of the iPP/10%Noryl/5% SEP blend revealed that SEP compatibilizer reduced the Noryl particle size down to about 0.3 μm (Fig. 6f). The 2% SEP compatibilized iPP/10%Noryl blend has a larger particle size ($\approx$0.8 μm) and a higher toughness than the 5% SEP modified iPP/10%Noryl blend [30]. To understand the differences and similarities in fracture mechanisms between the two blends, TOM, SEM and TEM investigations were further performed on iPP/10%Noryl/2%SEP.

The crack tip damage zone in DN-4PB iPP/10% Noryl/2%SEP is shown in Fig. 9. It is clear that the damage feature in 2% SEP compatibilized blend is similar to, but larger than, that of the 5% SEP compatibilized blend. Since the level of plastic deformation in the 2% SEP compatibilized blend is much higher, the evidence of fracture mechanisms at the crack tip cannot be retained after TEM thin-sectioning. As a result, the fracture mechanisms cannot be observed using TEM and instead, were investigated using SEM on an etched sub-fracture process zone.

The DN-4PB sub-fracture process zone was etched using an oxidizing acid agent described in the experimental section. The thermoplastic Noryl particles, SEP phase and materials inside the crazes were etched preferentially and could be easily revealed using SEM. It is important to point out here that the specimen is featureless under SEM before etching. The SEM photographs taken in the crack wake and the crack tip regions are shown in Figs 10 and 11. The particles are removed by the etching solution, leaving semi-spherical cavities that are connected by deeply etched crazes in the regions away from the fracture surface and the crack tip (Figs 10b and 11c). The removed particles and crazes form massive void line arrays. These void line arrays become narrow in the region close to the fracture surface (Fig. 10a) and are distorted at the crack tip (Fig. 11a and b). The general deformation feature in this blend is similar to that in 5% SEP compatibilized blend, i.e., crazing followed by shear banding. However, careful investigation reveals that the 2% SEP compatibilized blend exhibits more extensive crazing than that in 5% SEP compatibilized blend (Fig. 7c and d vs. Fig. 12a). The large Noryl particles ($\approx$0.8 μm) in the 2% SEP compatibilized blend (Fig. 12b) are more effective in triggering crazes than the small Noryl particles ($\approx$0.3 μm) in the 5% SEP compatibilized blend.

4. Discussion

The details of the toughening principles for polymers with rubber-toughened epoxy were discussed and

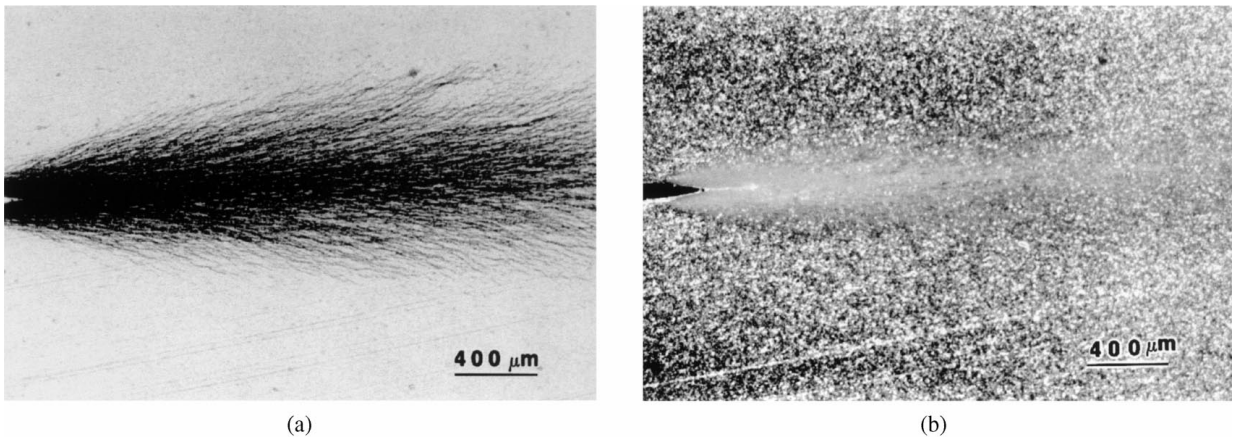

(a) (b)

Figure 9 TOM of DN-4PB iPP/10%Noryl/2%SEP specimen taken under (a) bright field and (b) cross-polarized light. The crack propagates from left to right.

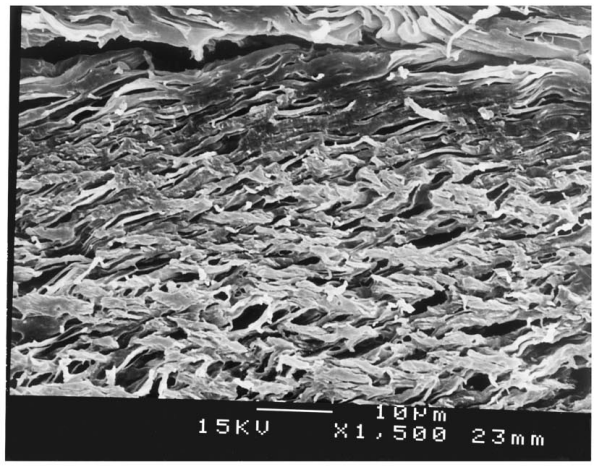

(a)

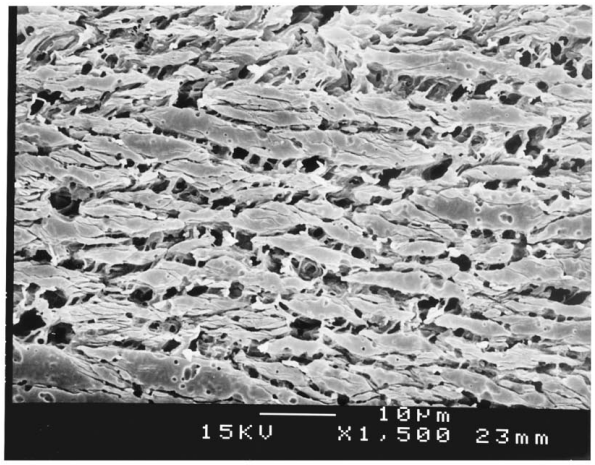

(b)

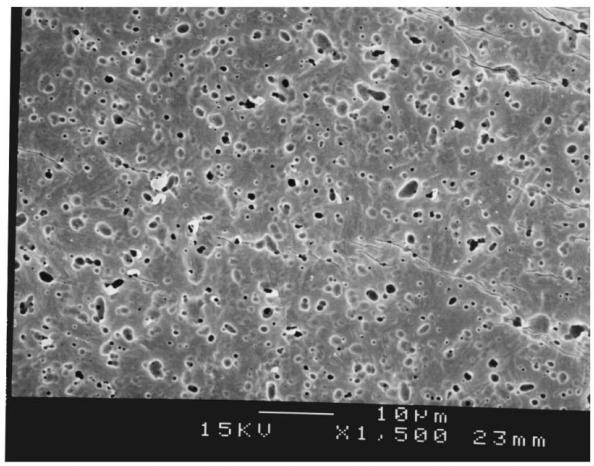

(c)

Figure 10 SEM micrographs of iPP/10%Noryl/2%SEP DN-4PB specimen taken in the crack wake. (a) Immediately beneath the crack surface, (b) 150 μm beneath the crack surface, and (c) undamaged region. Massive crazing (b) and shear banding (a) are observed. The crack propagates from left to right.

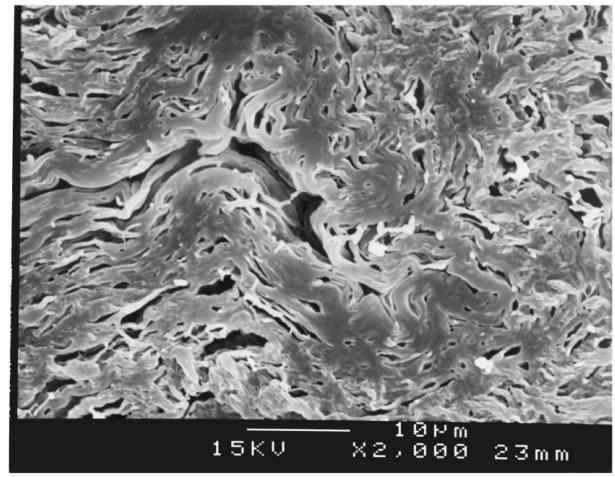

(a)

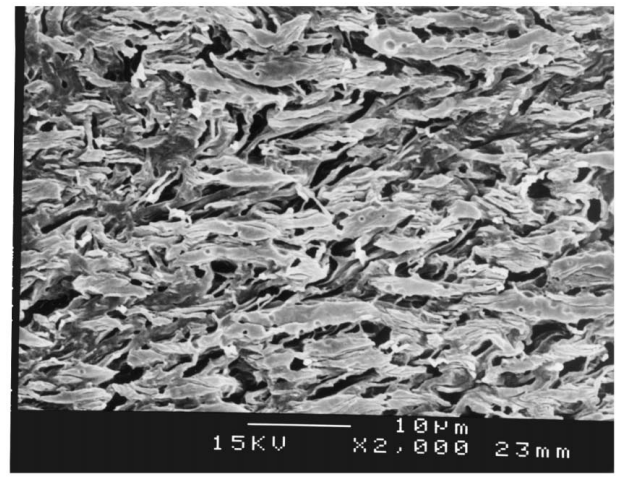

(b)

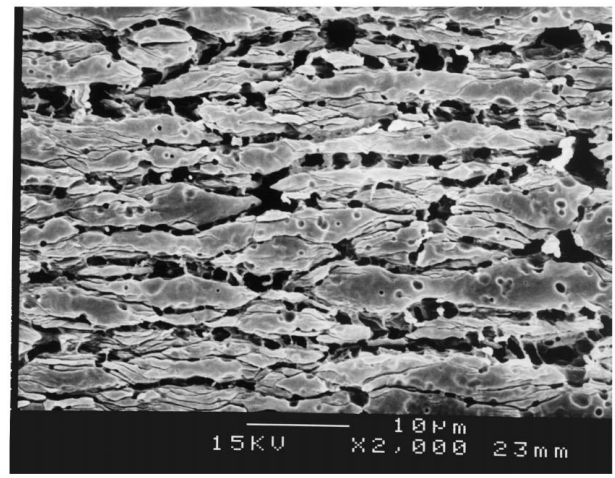

(c)

Figure 11 SEM micrographs of iPP/10%Noryl/2%SEP DN-4PB specimen taken in front of crack tip. (a) Crack tip, (b) 50 μm ahead of the crack tip, and (c) 800 μm ahead of the crack tip. The transformation of crazing (c) into shear banding (a, b) are observed. The crack propagates from left to right.

summarized by Yee and Pearson [16]. For rigid-rigid toughened polymers, Sue and Yee [3] demonstrated that toughness could be improved through crazing and transformation of crazing into shear banding in PA/PPO alloy. Studies on PBT/PC blends [28] showed another toughening route, i.e., crazing and debonding-cavitation at the PBT/PC interface, followed by matrix shear deformation. Unfortunately, the materials used in the above systems are commercial products, which makes it impossible to clearly determine the roles that the individual components play in the toughening process. The aim of this study is to obtain an unambiguous understanding of the roles played by individual constituents in the toughening process.

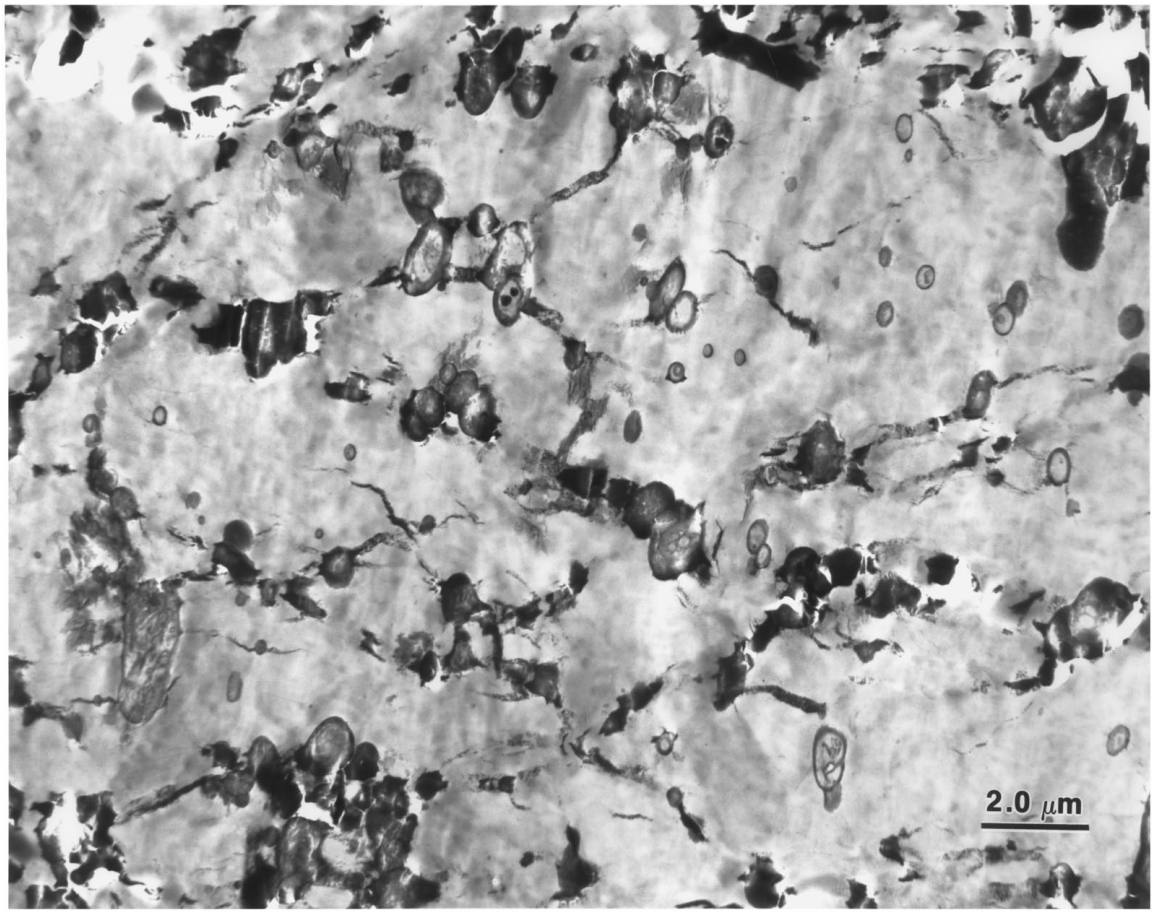

(a)

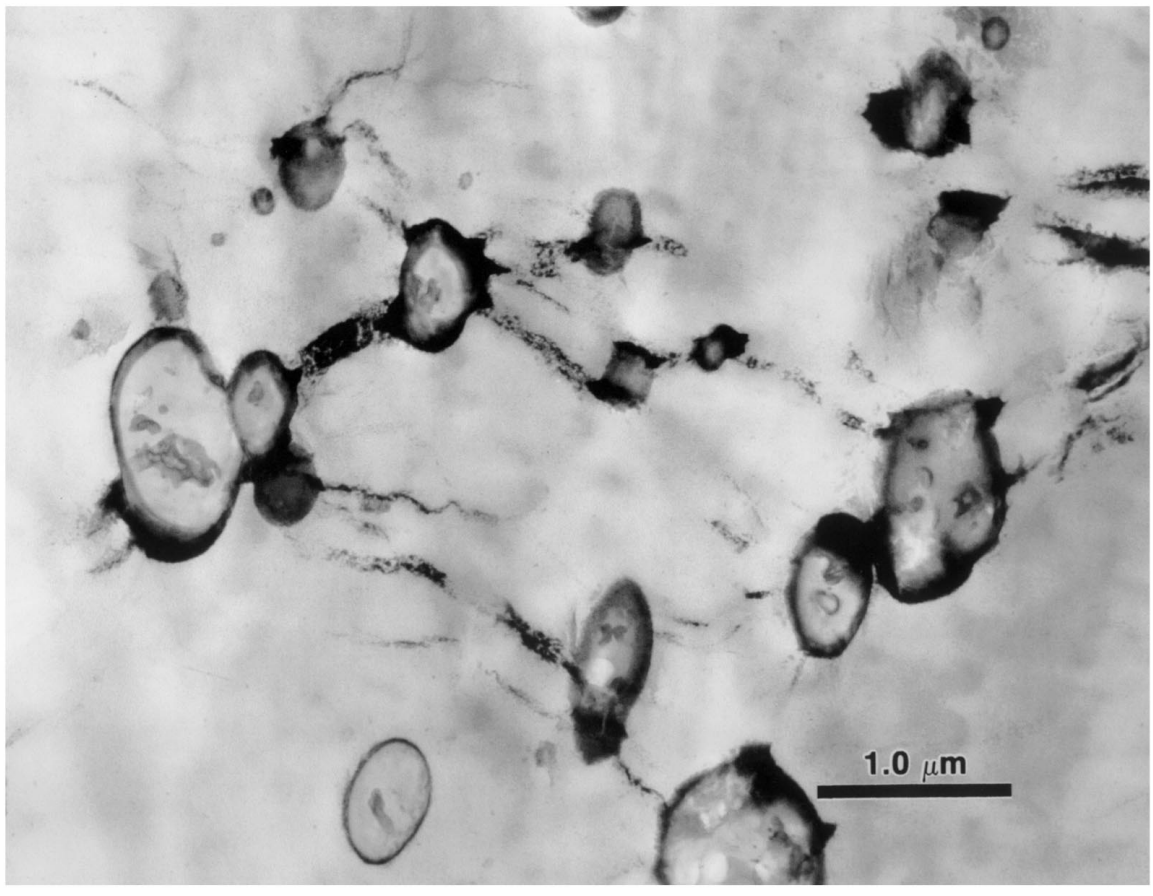

(b)

Figure 12 TEM of DN-4PB iPP/10%Noryl/2%SEP thin section taken at (a) 250 μm ahead of the crack tip, (b) high magnification of (a).

In iPP/10%Noryl blend, it is noted that Noryl particles have sizes ranging from 10–15 μm. These particles are effective in initiating and terminating crazes. The level of crazing is not sufficient to relieve triaxial stress constraint due to large inter-particle distances. In addition, the interfacial adhesion between Noryl particles and iPP matrix is not strong (Fig. 4a). With increased loading after matrix crazing, the debonding takes place. Subsequently, cracking ensues. As a result, the shear yielding mechanism is suppressed. We surmise that if the mixing is done at a higher temperature (e.g., 230 °C) and a higher level of Noryl particles is incorporated, smaller particles and shorter distance between particles could be achieved due to the reduced viscosity at high temperatures. By doing so, there is a good chance that the fracture mechanisms in iPP/Noryl blend may be transformed from being crazing dominant to crazing/matrix shear yielding dominant mechanisms. This will further increase the fracture toughness of the iPP/Noryl blend.

In the SEP-compatibilized iPP/Noryl blends, a higher SEP content reduces Noryl particle size but does not improve fracture toughness. In fact, the toughness measurement results showed that *Jc* value of iPP/10%Noryl/2%SEP blend is higher than that of iPP/10%Noryl/5%SEP blend [30]. This can be tentatively explained as follows. As is well known, the particle size plays an important role in toughening. It has been shown that large rubber particles (>1 μm) in HIPS and ABS are more effective in generating crazes than small particles [14, 34]. In rubber toughened PP, Jang [22] reported that samples with average particle diameter larger than 0.5 μm exhibited pronounced crazing while no craze was found in the sample with particles less than 0.5 μm. Donald and Kramer [14] and Bucknall [35] elaborated the reasons for large particles to be more effective in triggering crazes in polymer matrix. In the blends studied here, the average particle size in 2% SEP compatibilized blend is about 0.8 μm, while that in 5% SEP compatibilized blend is about 0.3 μm. Since a higher level of crazing and a larger crazed zone are generated in 2% SEP compatibilized blend, it is possible that the optimal particle size for triggering crazing in iPP is close to 0.8 μm.

High level of crazing may be responsible for a large shear banding zone in the 2% SEP compatibilized blend. To achieve shear banding, the plane strain constraint at crack tip has to be relieved by dilatational deformation. In rigid-rigid polymer blends, crazing is a main dilatational deformation process because cavitation of rigid particles is difficult. Therefore, the level of crazing is critical to the size of the shear yielded zone. A high level of crazing is more likely to relieve the triaxial stress at the crack tip. As a result, a larger shear yielded zone can be developed in iPP/10%Noryl/2%SEP (Fig. 9b).

The transformation of a crazed zone into a shear yielded zone in iPP/10%Noryl/SEP blends is observed in the present study. The similar phenomenon was previously described and the possible reasons for its occurrence were extensively discussed by Sue and Yee [3] in PA/PPO alloy. It should be pointed out that although the deformation phenomenon in these material systems is similar, the detailed toughening processes are different. One should note that PA/PPO alloy contains an elastomeric phase that initiates crazes inside the PPO particles. The crazes then propagate from the PPO particles into PA matrix. In the iPP/Noryl/SEP blends, the crazes are initiated by Noryl particles. No craze is found inside the Noryl particles. Studies have shown that crazing is the main fracture mechanism in neat iPP. This means that the stress level required for crazes to occur in iPP is lower than that for yielding to occur. The level of stress concentration at the equator of Noryl particles first reaches the required stress level to initiate crazes. With increasing loading, more crazes are generated and this relieves the triaxial stress at crack tip. These two processes enable shear yielding to occur easily.

Crack tip blunting mechanism has clearly operated in the iPP/Noryl/SEP blends. The TEM and SEM investigations of DN-4PB specimens (see Figs 7a and 11a) confirm that the iPP matrix is highly stretched around the crack tip, suggesting that plastic flow has occurred. As a result, the crack tip has been effectively blunted due to the surrounding plastically deformed material.

It is demonstrated that the rigid-rigid polymer toughening concept works well in Noryl particle toughened iPP. Toughness of the rigid polymer blends can be significantly increased through crazing or crazing/shear banding toughening mechanisms. One should note that the molecular structures of iPP and Noryl are very different, and Noryl particle has a much higher modulus and is more brittle than the matrix (iPP). The blend can still be tough. This provides an attractive route to improve both toughness and modulus of polymer matrix simultaneously. We surmise that this concept might work for all polymer blends so long as the effective toughening mechanisms, such as crazing and shear banding, can be achieved by properly controlling particle size and interfacial adhesion between the matrix and the toughener phase.

5. Conclusion

The toughening mechanisms in iPP, iPP/Noryl and iPP/Noryl/SEP blends have been examined using a variety of microscopy techniques. The results show that neat iPP undergoes brittle failure *via* unstable crazing. Noryl particles in iPPP/Noryl blend act as stress concentrators to trigger and stabilize crazes. Crazing is the dominant fracture toughening mechanism in iPP/Noryl blend. SEP compatibilizer, which reduces the Noryl particle size in iPP matrix and improves interfacial adhesion between iPP and Noryl particles, plays an important role in toughening. Addition of SEP transforms crazing dominant mechanism in iPP/10%Noryl into crazing/shear yielding mechanisms in iPP/10%Noryl/SEP blends.

Acknowledgements

The authors would like to thank GE Plastics and Shell Chemical for donating materials for the present work.

Special thanks are given to Defense Logistic Agency (Contract # SPO 103-96-D-0023) for the financial support of this work.

References

1. A. F. YEE, D. S. PARKER, H.-J. SUE and I.-C. HUANG, PMSE Div., Preprints, 194th ACS National Meeting, Aug. 1987.
2. H.-J. SUE and A. F. YEE, SPE-RETEC (Chicago), The Society of Plastics Engineers, Sept. 1987.
3. H.-J. SUE and A. F. YEE, *J. Mater. Sci*. **24** (1989) 1447.
4. *Idem., ibid.* **26** (1991) 3449.
5. H.-J. SUE, R. A. PEARSON and A. F. YEE, *Polym. Eng. Sci.* **31** (1991) 793.
6. M. HEINO, J. KIRJAVA, P. HIETAOJA and J. SEPPALA, *J. Appl. Polym. Sci.* **65** (1997) 241.
7. S. V. NAIR, S.-C. WONG and L. A. GOETTLER, *J. Mater. Sci.* **32** (1997) 5335.
8. S. V. NAIR and A. SUBRAMANIAM, *ibid.* **32** (1997) 5347.
9. *Idem., ibid.* **33** (1998) 3455.
10. R. P. KAMBOUR, *J. Polym. Sci., Macromol Rev.* **7** (1973) 1.
11. C. B. BUCKNALL, D. CLAYTON and W. E. KEAST, *J. Mater. Sci.* **7** (1972) 1443.
12. A. M. DONALD, E. J. KRAMER and R. P. KAMBOUR, *ibid.* **17** (1982) 1739.
13. R. R. DURST, R. M. GRIFFITH, A. J. URBANIC and W. J. VAN ESSEN, *ACS Div. Org. Coat. Plast. Prepr*. **34** (1974) 320.
14. A. M. DONALD and E. J. KRAMER, *J. Appl. Polym. Sci*. **27** (1982) 3729.
15. C. B. BUCKNALL, "Toughened Plastics" (Applied Science, London, 1977).
16. A. F. YEE and R. A. PEARSON, *J. Mater. Sci.* **21** (1986) 2462.
17. *Idem., ibid.* **21** (1986) 2475.
18. H. G. OLF and A. PETERLIN, *J. Polym. Sci., Polym. Phys.* **12** (1974) 2209.
19. R. GRECO and G. RAGOSTA, *J. Mater. Sci.* **23** (1988) 4171.
20. M. SUGIMOTO, M. ISHIKAWA and K. HATADA, *Polymer* **36** (1995) 3675.
21. B. Z. JANG, D. R. UHLMANN and J. B. VANDER SANDE, *J. Appl. Polym. Sci.* **30** (1985) 2485.
22. *Idem., Polym. Eng. Sci.* **25** (1985) 643.
23. J. KARGER-KOCSIS and I. CSIKAI, *ibid.* **27** (1987) 241.
24. M. ISHIKAWA, M. SUGIMOTO and T. INOUNE, *J. Appl. Polym. Sci.* **62** (1996) 1495.
25. C. J. CHOU, K. VIJAYAN, D. KIRBY, A. HILTNER and E. BAER, *J. Mater. Sci.* **23** (1988) 2521.
26. *Idem., ibid.* **23** (1988) 2533.
27. D. E. MOUZAKIS, F. STRICKER, R. MULHAUPT and J. KARGER-KOCSIS, *ibid.* **33** (1998) 2551.
28. J. S. WU and Y.-W. MAI, *ibid.* **28** (1993) 6167.
29. B. MAJUMDAR, H. KESKKULA and D. R. PAUL, *J. Polym. Sci. Part B, Polym. Phy.* **32** (1994) 2127.
30. G.-X. WEI and H.-J. SUE, *Polymer*, in Press.
31. A. S. HOLIK, R. P. KAMBOUR, S. Y. HOBBS and D. G. FINK, *Microstruct. Sci*. **7** (1979) 357.
32. R. H. OLLEY and D. C. BASSET, *Polymer* **23** (1983) 1707.
33. D. C. BASSET and R. H. OLLEY, *ibid.* **25** (1984) 935.
34. *Idem., J. Mater. Sci.* **13** (1982) 1765.
35. C. B. BUCKNALL, *ibid.* **4** (1969) 214.

Received 13 April
and accepted 4 May 1999